

# A flexible sequential Monte Carlo algorithm for shape-constrained regression

Kenyon Ng<sup>a,\*</sup>, Kevin Murray<sup>b,c</sup>, Berwin A. Turlach<sup>a,c</sup>

<sup>a</sup>*School of Mathematics and Statistics (M019), The University of Western Australia,  
35 Stirling Highway, Crawley WA 6009*

<sup>b</sup>*School of Population and Global Health (M431), The University of Western Australia,  
35 Stirling Highway, Crawley WA 6009*

<sup>c</sup>*Centre for Applied Statistics (M019), The University of Western Australia, 35 Stirling  
Highway, Crawley WA 6009*

---

## Abstract

We propose an algorithm that is capable of imposing shape constraints on regression curves, without requiring the constraints to be written as closed-form expressions, nor assuming the functional form of the loss function. Our algorithm, which is based on Sequential Monte Carlo-Simulated Annealing, only relies on an indicator function that assesses whether or not the constraints are fulfilled, thus allowing us to enforce various complex constraints by specifying an appropriate indicator function without altering other parts of the algorithm. We demonstrate our algorithm by fitting rational function models subject to monotonicity and continuity constraints. The algorithm was implemented using R (R Core Team, 2018) and the code is freely available on GitHub.

*Keywords:* shape constraints, constrained optimisation, simulated

---

\*Corresponding author

*Email addresses:* [kenyon.ng@research.uwa.edu.au](mailto:kenyon.ng@research.uwa.edu.au) (Kenyon Ng),  
[kevin.murray@uwa.edu.au](mailto:kevin.murray@uwa.edu.au) (Kevin Murray), [berwin.turlach@gmail.com](mailto:berwin.turlach@gmail.com) (Berwin A. Turlach)

## 1. Introduction

Shape constraints, such as monotonicity or convexity, can be required on a regression curve to ensure its interpretability due to some external theory. For instance, growth curve modelling often requires monotonicity constraints to be imposed on the response curve (Marsh, 1980; Thornley, 1999), or shape constrained models can be used to estimate dose-response curves (Kelly and Rice, 1990), cumulative distribution functions (Ramsay, 1998) and various response curves in economics that are convex by some underlying theory (Matzkin, 1991). Therefore, fitting a shape-constrained regression model becomes a constrained optimisation problem, where the parameter space of the regression coefficients is appropriately restricted.

Despite the importance of restricting the shape of the regression curves, current shape constrained models are mainly concentrated on polynomial or spline models due to their relative ease of implementation. For instance, when considering monotonicity in polynomial models, apart from directly minimising the loss function subject to a restricted parameter space (Bon et al., 2017), such constraints can be achieved through an appropriate model parameterisation (Elphinstone, 1983; Murray et al., 2013, 2016; Manderson et al., 2017). On the other hand, when using penalised splines, the monotonicity or convexity conditions for models with truncated power series bases (up to quadratic spline) or B-spline bases can be written as a system of linear inequality constraints (Leitenstorfer and Tutz, 2007; Brezger and Steiner, 2008; Hazelton and Turlach, 2011; Meyer et al., 2011; Meyer, 2012; Pya and

Wood, 2015). However, shape-constrained models other than these are less common, partly due to the difficulty of deriving appropriate closed-form expressions required for enforcing the constraints. This motivates us to develop a flexible method that is capable of imposing shape constraints on a wide variety of regression models, even in the absence of closed-form expressions of the constraints.

We propose a new constrained optimisation method that works on any constraints that are presentable as an indicator function. Such constraints are not enforced by exploiting the mathematical expressions that describe them; rather, the feasibility of an estimate is only known from the indicator function. Consequently, our method is more versatile than those that assume specific structures on the constraints. To our knowledge, the only other optimisation method developed with the black-box constraint property is the constrained estimation particle swarm optimisation (CEPSO, Wolters, 2012) algorithm. However, CEPSO requires a pilot estimate to operate, which is usually the unconstrained global minimum. Since the unconstrained global minimum is often difficult to obtain, especially when there are multiple local minima in the loss function, there are some circumstances when CEPSO may be unsuitable. Our method is based on Sequential Monte Carlo-Simulated Annealing (SMC-SA, Zhou and Chen, 2013), and will overcome the need for a pilot estimate.

The remainder of the paper is outlined as follows: In Section 2, we will formally define the optimisation problem and discuss the challenges of solving this. The details of the constraint-augmented SMC-SA are discussed in Section 3. In Section 4, the performance of our method will be assessed by

fitting regression models on simulated datasets. We conclude and discuss our algorithm in Section 5.

## 2. Problem specification

Constrained regression analysis is usually analogous to finding a *state*  $\boldsymbol{\theta}^* \in \mathcal{S} \subset \mathbb{R}^d$ , where the feasible set  $\mathcal{S}$  is not necessarily finite or convex, such that a *loss function*  $f : \mathbb{R}^d \rightarrow \mathbb{R}$  is minimised

$$f(\boldsymbol{\theta}^*) \leq f(\boldsymbol{\theta}) \quad \text{for all } \boldsymbol{\theta} \in \mathcal{S}.$$

For the purpose of this study, we assume that  $\boldsymbol{\theta}^*$  is unique.

The classic approach of solving constrained optimisation problems is to introduce Lagrange multipliers into the loss function, and solve the system of equations attained from partially differentiating the transformed function with respect to the parameters and Lagrange multipliers (see for example Nocedal and Wright, 2006). In the usual case of minimising a complicated loss function, iterative algorithms may be the more sensible choice (see for example Romeijn and Smith, 1994; Andreani et al., 2013; Reddi et al., 2015).

However, most of the existing constrained optimisation methods are restricted to only solving problems with particular types of constraints, and are consequently not suitable for the development of a flexible constrained optimisation methodology. Moreover, there are constraints which cannot be written down as a finite set of closed-form expressions. For example, fitting a least squares continuous rational function requires its denominator polynomial to be non-zero over the region of interest, implying that there are infinitely many non-equalities to be considered. It is therefore difficult, if not impossible, to implement any of the traditional methods for this problem.

### 3. Optimisation

It is well known that the Boltzmann distribution of the form

$$\pi(\boldsymbol{\theta}) \propto \exp \left\{ -\frac{f(\boldsymbol{\theta})}{T} \right\}$$

will converge to a degenerate distribution whose mass is concentrated on the global minimum of  $f(\boldsymbol{\theta})$  when the temperature  $T$  converges to 0. Similarly for constrained optimisation problems, it can be shown that this will still hold when the solution space is restricted, that is

$$\pi(\boldsymbol{\theta}) \propto \exp \left\{ -\frac{f(\boldsymbol{\theta})}{T} \right\} \mathbb{1}_{\mathcal{S}}, \quad (1)$$

where  $\mathbb{1}_{\mathcal{S}}$  is an indicator for  $\boldsymbol{\theta} \in \mathcal{S}$ , will converge to a degenerate distribution concentrated on the constrained global minimum  $\boldsymbol{\theta}^*$  (Romeijn and Smith, 1994). In light of these results, a constrained optimisation problem can essentially be solved by drawing samples from (1) with  $T \rightarrow 0$ , a fact employed by the algorithm we are proposing.

#### 3.1. Simulated annealing

The Metropolis algorithm (Metropolis et al., 1953), a Markov chain Monte Carlo (MCMC) technique, can be employed to draw samples from (1), in a similar fashion to simulated annealing (Kirkpatrick et al., 1983; Locatelli, 2000). More specifically, we sample from a sequence of Boltzmann distributions

$$\pi_k(\boldsymbol{\theta}) \propto \exp \left\{ -\frac{f(\boldsymbol{\theta})}{T_k} \right\} \mathbb{1}_{\mathcal{S}}, \quad k = 1, 2, 3 \dots \quad (2)$$

that starts from a Boltzmann distribution with high temperature and eventually converges to the degenerate distribution of interest (i.e.  $T_k \rightarrow 0$ ).

Simulated annealing first simulates a Markov chain with invariant  $\pi_1$ , then proceeds to simulate the rest of  $\pi_k$  with fresh Markov chains using the sample from the preceding  $\pi_{k-1}$  as starting values. This construction of sampling from a distribution sequence, rather than direct sampling from (1) with low  $T$ , is necessary to facilitate efficient sampling due to the low acceptance probability of Markov chain when the temperature is low. This can be observed evidently from the formula of the acceptance probability for each  $\pi_k$

$$p_k = \min \left\{ 1, \exp \left\{ -\frac{f(\tilde{\boldsymbol{\theta}}) - f(\boldsymbol{\theta}_{k-1})}{T_k} \right\} \mathbb{1}_{\mathcal{S}} \right\}, \quad (3)$$

where  $\tilde{\boldsymbol{\theta}}$  and  $\boldsymbol{\theta}_{k-1}$  denote proposed and previous states respectively. At low temperature, even a small difference of  $f(\boldsymbol{\theta})$  will lead to the exponential function being evaluated at large negative values.

Since simulated annealing minimises  $f(\boldsymbol{\theta})$  by sampling from (2), there are two decisions to be made: the number of samples drawn from  $\pi_k$  before moving to  $\pi_{k+1}$ , and the choice of temperature  $T_k$  at each iteration. Naturally when sampling from  $\pi_k$ , the ideal situation will be simulating its corresponding Markov chain until the invariant distribution of the chain is achieved, and using the sample from  $\pi_k$  as the starting state of the subsequent Markov chain to sample from  $\pi_{k+1}$ . This strategy is clearly impractical in general due to a large amount of transitions required for each Markov chain to achieve stationarity; rather, the common practice is to perform only a single transition for each  $k$ . Consequently, those Markov chains never achieve their stationarity, and some conditions (such as the choice of  $T_k$  and the proposal distribution) have to be followed to ensure that the whole algorithm will still minimise  $f(\boldsymbol{\theta})$  when  $k \rightarrow \infty$  (Locatelli, 2000). For more detailed analysis

and implementation of constrained simulated annealing with compact  $\mathcal{S}$ , we refer to Romeijn and Smith (1994) and Locatelli (2002).

While simulated annealing will converge to the global minimum when  $k \rightarrow \infty$ , in practice one can only carry out a finite number of iterations. This may lead the algorithm to converge to a local minimum if it starts from a poor state and stops prematurely. However, with the abundance of parallel computing power available nowadays, this issue can be mitigated by performing multiple independent simulated annealings that start from different states. For the rest of this paper, we will refer to this technique as multi-start SA, which starts from  $N$  different locations, leading to the following set of search chains  $\{\boldsymbol{\theta}_k^j\}_{k=0}^K, j = 1, 2, \dots, N$  after  $K$  iterations. Arguably, this strategy of starting from multiple states is widely used by practitioners when multiple local minima are present in the loss function, in the hope that at least one of the search chains will converge to the global minimum. As we will argue in the following, multi-start SA can be improved by utilising the information extracted from  $\{\boldsymbol{\theta}_k^j\}_{j=1}^N$  at each iteration, which is the motivation of SMC-SA.

### *3.2. Sequential Monte Carlo-Simulated Annealing*

An alternative approach to sample from (2) is the Sequential Monte Carlo (SMC) sampler proposed by Del Moral et al. (2006) and formalised by Zhou and Chen (2013) some years later, who then called the resulting algorithm Sequential Monte Carlo-Simulated Annealing (SMC-SA). Intuitively speaking, SMC-SA is a multi-start SA algorithm combined with the idea of importance sampling. Prior to the start of Markov transitions at each iteration, the importance sampling step will only select the states with lower objective

function values for further optimisation, and discard the rest to save computational resources. From a MCMC perspective, all states  $\{\boldsymbol{\theta}_{k-1}^j\}_{j=1}^N$  are weighted and sampled at the start of each iteration to resemble  $\pi_k$  before performing Markov transition, such that the single-transition Markov chain can achieve its invariant distribution (i.e.  $\pi_k$ ) more easily.

We will discuss SMC-SA as a two-step process, namely importance sampling and the SA-move.

1. Importance sampling: The idea of the importance sampling step is to filter out states with greater objective function values, which are less likely to lead to the global minimum. This is implemented by sampling  $N^*$  *promising states*  $\{\boldsymbol{\gamma}_k^j\}_{j=1}^{N^*}$  from the pool of  $N$  previous states  $\{\boldsymbol{\theta}_{k-1}^j\}_{j=1}^N$  at the start of each iteration, according to the weights  $\{w_k^j\}_{j=1}^N$  assigned to each  $\boldsymbol{\theta}_{k-1}^j$

$$w_k^j \propto \begin{cases} \exp\left\{-\frac{f(\boldsymbol{\theta}_0^j)}{T_1}\right\}, & k = 1; \\ \exp\left\{-f(\boldsymbol{\theta}_{k-1}^j)\left(\frac{1}{T_k} - \frac{1}{T_{k-1}}\right)\right\}, & k > 1. \end{cases} \quad (4)$$

The eventual output from the importance sampling step is a set  $\{\boldsymbol{\gamma}_k^j\}_{j=1}^{N^*}$ .

2. SA-move (Markov kernel): The  $\{\boldsymbol{\gamma}_k^j\}_{j=1}^{N^*}$  from the importance sampling step are then transitioned once with a Markov kernel with invariant distribution of  $\pi_k$ . For each  $\boldsymbol{\gamma}_k^j$ , a candidate state is drawn from a symmetrical random walk proposal  $q(\boldsymbol{\theta}|\boldsymbol{\theta}_{k-1}^j)$  which is centred on  $\boldsymbol{\theta}_{k-1}^j$ , and performs an accept-reject routine according to (3) to determine  $\boldsymbol{\theta}_k^j$ . This step is essentially performing an iteration of the Metropolis algorithm with  $\boldsymbol{\gamma}_k^j$  as the starting value.

The pseudocode of SMC-SA is outlined in Algorithms 1 and 2.

---

**Algorithm 1** SA-Move (Markov kernel  $K_k(\boldsymbol{\theta}_{k-1}, \boldsymbol{\theta}_k)$ )

---

- 1: **procedure** SA-MOVE( $\boldsymbol{\theta}_{k-1}, T_k$ )
  - 2:    $\tilde{\boldsymbol{\theta}} \leftarrow$  A sample from  $q(\boldsymbol{\theta}|\boldsymbol{\theta}_{k-1})$ .
  - 3:    $p_k \leftarrow$  Evaluate (3).
  - 4:    $u \leftarrow$  A sample from  $Uniform(0, 1)$ .
  - 5:    $\boldsymbol{\theta}_k \leftarrow \begin{cases} \tilde{\boldsymbol{\theta}} & \text{if } u \leq p_k; \\ \boldsymbol{\theta}_{k-1} & \text{otherwise.} \end{cases}$
  - 6:   **return**  $\boldsymbol{\theta}_k$
  - 7: **end procedure**
- 

### 3.2.1. Proposal distribution

The selection of  $q(\boldsymbol{\theta}|\boldsymbol{\theta}_{k-1})$  can greatly affect the transition of the chain, and thus the quality of the samples being drawn. More specifically, a proposal distribution with significant mass outside  $\mathcal{S}$  will result in the chain rarely moving to a new state. In this case, a random walk proposal with support  $\mathcal{S}$ , which we refer to as truncated random walk for the remainder of this paper, will be a more ideal candidate than a symmetrical random walk, as it ensures the acceptance probability to be strictly positive. Using a proposal other than a symmetrical random walk also implies that (3) needs to be adjusted with a ratio of proposal densities evaluated at the current and proposed states (Hastings, 1970)

$$p_k = \min \left\{ 1, \frac{q(\tilde{\boldsymbol{\theta}}|\boldsymbol{\theta}_{k-1})}{q(\boldsymbol{\theta}_{k-1}|\tilde{\boldsymbol{\theta}})} \exp \left\{ -\frac{f(\tilde{\boldsymbol{\theta}}) - f(\boldsymbol{\theta}_{k-1})}{T_k} \right\} \mathbb{1}_{\mathcal{S}} \right\}, \quad (5)$$

---

**Algorithm 2** Sequential Monte Carlo-Simulated Annealing

---

```
1: procedure SMC-SA( $\{\theta_0^j\}_{j=1}^N$ )
2:    $k \leftarrow 1$ .
3:   repeat
4:      $T_k \leftarrow T(k)$ 
5:      $\{w_k^j\}_{j=1}^N \leftarrow$  Evaluate (4)
6:      $\{\gamma_k^j\}_{j=1}^{N^*} \leftarrow$  Resample from  $\{\theta_{k-1}^j\}_{j=1}^N$ , with weights  $\{w_k^j\}_{j=1}^N$ .
7:     for  $j = 1, 2, 3, \dots, N^*$  do
8:        $\theta_k^j \leftarrow$  SA-MOVE( $\gamma_k^j, T_k$ )
9:       if  $f(\theta_k^j) < f(\theta^*)$  then  $\theta^* \leftarrow \theta_k^j$ 
10:      end if
11:    end for
12:     $k \leftarrow k + 1, N \leftarrow N^*$ 
13:  until Stopping criterion is met.
14: end procedure
```

---

to preserve the reversibility of the Markov kernel. However, the calculation of (5) is not trivial.

Since our end goal is not to sample from the Boltzmann distributions, but merely use them as a vehicle to minimise  $f(\boldsymbol{\theta})$ , our aim can be achieved as long as the global minimum is visited once by the algorithm. Therefore, we ignore the proposal ratio in (5) and use (3) to calculate acceptance probabilities.

Sampling from a truncated random walk, especially when the nature of constraint is unknown, is a difficult problem and we have to resort to a rejection sampler. In our algorithm, we employ a truncated normal random walk proposal

$$q(\boldsymbol{\theta}|\boldsymbol{\theta}_{k-1}) = c(\boldsymbol{\theta}_{k-1}) \exp \left\{ \frac{1}{2\sigma^2} \|\boldsymbol{\theta} - \boldsymbol{\theta}_{k-1}\|^2 \right\} \mathbb{1}_{\mathcal{S}}, \quad (6)$$

where  $c(\boldsymbol{\theta}_{k-1})$  is a normalising constant dependent on  $\boldsymbol{\theta}_{k-1}$ , and  $\sigma^2$  is set to decrease gradually after each iteration. This distribution can be sampled (albeit inefficiently) by repeatedly sampling from its corresponding normal distribution  $N(\boldsymbol{\theta}_{k-1}, \sigma^2 \mathbf{I})$  until a sample coming from  $\mathcal{S}$  is obtained.

### 3.2.2. Cooling schedule

A cooling schedule is a function that controls the temperature at each iteration, which in turn affects the algorithm convergence. It should restrict the cooling rate such that the invariant distributions of adjacent Markov chains do not differ too much, and the initial states for each chain in (2) are more likely to fall within the high density region of their respective invariant distributions. The choice of cooling schedule is usually dependent on the problem at hand.

There are two conditions to meet for SMC-SA to converge:  $T_k \rightarrow 0$  and  $\left| \frac{1}{T_k} - \frac{1}{T_{k-1}} \right|$  is monotonically decreasing (Zhou and Chen, 2013). Schedules that satisfy both of these conditions include the *logarithm schedule*, which is suggested in Zhou and Chen (2013) and has the form

$$T(k) = \frac{|f(\boldsymbol{\theta}_k^*)|}{\log(k+1)},$$

where  $\boldsymbol{\theta}_k^*$  is the best state observed up until the  $k^{\text{th}}$  iteration. However, as described in Nourani and Andresen (1998), the cooling rate of the logarithm schedule can be too conservative, and an alternative is to use a more stringent *reciprocal schedule*

$$T(k) = \frac{|f(\boldsymbol{\theta}_k^*)|}{1 + \alpha(k-1)^2}, \quad 0 < \alpha < 1. \quad (7)$$

In our experience, this schedule outperforms the logarithm schedule when using our modified SMC-SA algorithm in terms of the best minimum achieved for a given number of iterations, despite  $\left| \frac{1}{T_k} - \frac{1}{T_{k-1}} \right|$  not being monotonically decreasing.

### 3.2.3. SMC-SA and SMC sampler

The SMC-SA algorithm can also be seen as a special case of the SMC sampler (Del Moral et al., 2006) that simulates the distribution sequence in (2) with the following specifications:

- the initial distribution is  $\pi_0(\boldsymbol{\theta}) \propto 1$ ;
- Metropolis MCMC forward kernels  $K_k(\boldsymbol{\theta}_{k-1}, \boldsymbol{\theta}_k)$  are used with invariant distributions given by (2);

- the backward kernels are

$$L_{k-1}(\boldsymbol{\theta}_k, \boldsymbol{\theta}_{k-1}) = \frac{\pi_k(\boldsymbol{\theta}_{k-1})K_k(\boldsymbol{\theta}_{k-1}, \boldsymbol{\theta}_k)}{\pi_k(\boldsymbol{\theta}_k)},$$

- states are resampled after each iteration to avoid degeneracy.

In this case, Equation (4) gives the weights for each sample in the SMC sampler. The implementation of  $K_k(\boldsymbol{\theta}_{k-1}, \boldsymbol{\theta}_k)$  is outlined in Algorithm 1.

#### 4. Applications

In this section, we will discuss the convergence performance of our constraint-augmented SMC-SA and compare it to CEPSO which serves as our benchmark. We demonstrate our algorithm by fitting rational function models subject to monotonicity and continuity constraints using both least squares and Tukey’s biweight loss functions. In all of these applications, the SMC-SA algorithm used 400 iterations and a reciprocal schedule, with the hyperparameter  $\alpha$  in (7) set to 0.85, which was determined through extensive numerical trials. The  $\sigma^2$  in (6) was set to 1 initially and decreased by 3% after each iteration. The sample size  $N^*$  at the importance sampling step was fixed throughout the algorithm (i.e.  $N^*$  equals to the number of starting values).

For CEPSO, the algorithm used 2000 iterations, and the neighbourhood size for local best estimation was set to 200. The methods for obtaining starting values and pilot estimates are problem-specific and will be discussed in the later sub-sections. However, all algorithms were started from 1000 different locations in the feasible space  $\mathcal{S}$ , and were repeated 100 times to observe the variations between the results from each run. This simulation study was conducted in R (R Core Team, 2018).

#### 4.1. Rational function models

Rational functions are fractions whose numerator and denominator are both polynomials. They are usually more flexible than polynomials in the sense that they can describe a given curve with fewer parameters, yet retaining the same degree of accuracy (Newman, 1964; Ralston and Rabinowitz, 1978). Apart from their superior flexibility, some physical phenomena can be precisely modelled as a rational function, such as the Michaelis-Menten kinetics model in biochemistry (Piegorsch and Bailer, 2005). However, rational function models are not continuous at the roots of their denominator, making it challenging to reliably fit them to data in practical applications; see Figure 2.

We first consider a dataset generated from a hyperbolic tangent which has a sigmoidal shape

$$\text{HT0 : } Y_i = 1 + \tanh(x_i - 3) + \epsilon_i$$

where  $x_i = \frac{6}{29}(i - 1)$  and  $\epsilon_i \stackrel{i.i.d.}{\sim} N(0, 0.3^2)$ ,  $i = 1, \dots, 30$ . Our objective is to fit the following rational function model

$$y = r(x) = \frac{p_1(x)}{p_2(x)} = \frac{\beta_1 + \beta_2 x}{1 + \beta_3 x + \beta_4 x^2} \quad (8)$$

to the HT0 dataset, subject to both increasing monotonicity and continuity constraints in the interval  $[0, 6]$ . The necessary conditions for these constraints are

$$\begin{aligned} r'(x) &\geq 0 \\ \implies p_1'(x)p_2(x) - p_1(x)p_2'(x) &\geq 0, \quad \forall x \in [0, 6] \end{aligned} \quad (9)$$

and

$$p_2(x) \neq 0, \quad \forall x \in [0, 6], \quad (10)$$

where (9) and (10) are required for increasing monotonicity and continuity respectively. Although both (9) and (10) are not closed-form expressions, these conditions can be verified easily. For (9), the left hand side of the inequality, which itself is a polynomial, needs to fulfil two conditions: (i) all roots of the polynomial in  $[0, 6]$  must have even multiplicities; and (ii) the polynomial must be evaluated to a positive number at an arbitrary  $x$  in  $[0, 6]$ . To verify (10), we only need to ensure that the polynomial  $p_2(x)$  does not have any roots in  $[0, 6]$ .

The least squares estimate of (8) was estimated by minimising the model's residual sums of squares  $\text{RSS}(\boldsymbol{\theta})$

$$\text{RSS}(\boldsymbol{\theta}) = \sum_{i=1}^{30} (y_i - r(x_i; \boldsymbol{\theta}))^2, \quad \boldsymbol{\theta} \in \mathcal{S}, \quad (11)$$

where  $\boldsymbol{\theta} = (\beta_1, \beta_2, \beta_3, \beta_4)^T$ . The set of starting values  $\{\boldsymbol{\theta}_0^j\}_{j=1}^{1000}$  was sampled from a multivariate Cauchy( $\boldsymbol{\eta}_0, 2$ ) truncated to  $\mathcal{S}$  using a rejection sampler, where  $\boldsymbol{\eta}_0 \in \mathbb{R}^4$  is a least squares estimate acquired from regressing a linear model rearranged from (8)

$$y = \beta_1 + \beta_2 x - \beta_3 xy - \beta_4 x^2 y. \quad (12)$$

The pilot estimate for CEPSO was an unconstrained least squares estimate, which was obtained by minimising (11) with the Newton-Gauss algorithm and starting from  $\boldsymbol{\eta}_0$ .

Apart from SMC-SA with the reciprocal schedule and CEPSO, we also examined all the previously described algorithm-schedule combinations (i.e. multi-start SA and the logarithm schedule) in this example to show the differences

in performance, and justify the choice of using the reciprocal schedule. Table 1 shows that the SMC-SA with the reciprocal schedule clearly outperformed the rest of the SA-based algorithm combinations and is comparable to CEPSO. In particular, we can see that the results from CEPSO and SMC-SA with the reciprocal schedule did not vary greatly, and returned a good estimate of  $\theta^*$  in all of the 100 runs. In contrast, multi-start SA struggled to find the optimal solution with either schedule, and although SMC-SA with the logarithm schedule did converge to a close to optimal solution at least once, most of the time the algorithm failed to yield reasonable estimates.

The 100 regression curves produced by each algorithm-schedule combination are illustrated in Figure 1. Since the results produced by SMC-SA with the reciprocal schedule (middle right panel) and CEPSO (bottom panel) in each run did not differ greatly, their regression curves (grey) are overlaying one another, and thus appear to be a single curve. Conversely, the plots corresponding to the remaining algorithm-schedule combinations have a band-like structure due to large variability in the regression curves between each run. The pilot estimate for CEPSO (black dotted) is also shown in Figure 1 to serve as a reference. From these results and other extensive similar simulations (not reported here), we conclude that SMC-SA with the reciprocal schedule and CEPSO produce comparable and reliable estimates.

#### *4.2. Constrained robust models*

Observed data are sometimes contaminated with outliers, and a different loss function can be used to reduce their influence on the model fit. In this example, we demonstrate that our algorithm is capable of estimating the regression coefficients of (8), subject to both (9) and (10), with an M-

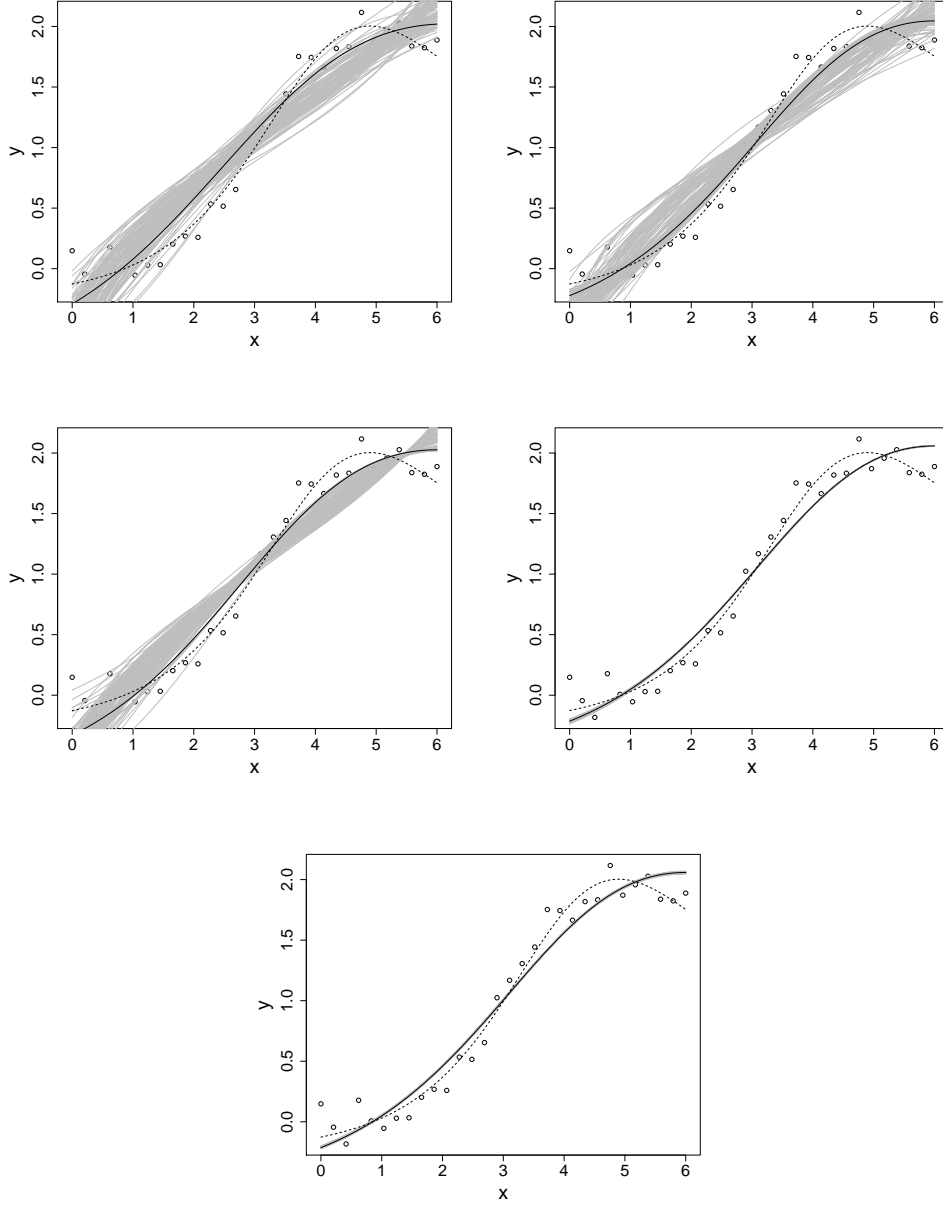


Figure 1: A hundred regression curves (grey) are plotted for each of the algorithm combination. The pilot estimate for CEPSO (black dotted) and the best estimate obtained from each algorithm (black solid) are shown. The plots on the left and right panels correspond to multi-start SA and SMC-SA respectively, while the top and middle panels correspond to the logarithm and reciprocal schedules respectively. The output from CEPSO is shown on the bottom panel.

Table 1: Mean, standard deviation, extremes, and quartiles of the objective values for 100 repeated runs of different algorithms and schedules, on HT0.

Algorithms		Mean	SD	Min	Q1	Q2	Q3	Max
Multi-SA	logarithm	2.660	0.526	1.117	2.391	2.737	3.071	3.738
	reciprocal	2.099	0.530	0.916	1.825	2.122	2.444	3.204
SMC-SA	logarithm	1.975	1.005	0.828	0.932	1.941	2.825	4.026
	reciprocal	0.827	0.001	0.826	0.826	0.826	0.827	0.829
CEPSO		0.827	0.001	0.826	0.826	0.827	0.827	0.829

estimator (Huber, 1981) which minimises the following loss function

$$f(\boldsymbol{\theta}) = \sum_{i=1}^{30} \rho(y_i - r(x_i; \boldsymbol{\theta})), \quad \boldsymbol{\theta} \in \mathcal{S}, \quad (13)$$

where  $\rho(\cdot)$  is carefully chosen to limit the influence of outliers on the overall model fit. The least squares estimator is essentially a special case of (13) where  $\rho(u) = u^2$ , but this particular choice of  $\rho(\cdot)$  greatly inflates the influence of outliers. Here, we employ Tukey’s biweight loss function

$$\rho(u) = \begin{cases} \frac{c^2}{6} \left( 1 - \left( 1 - \left( \frac{u}{c} \right)^2 \right)^3 \right), & |u| \leq c, \\ 1, & |u| > c, \end{cases}$$

where the choice of  $c$  is arbitrary, but our default value is 4.685.

In this example, we used a dataset purposefully contaminated with outliers. This dataset will be referred to as HT1, and was produced by setting the values of  $y_2$  and  $y_{28}$  in HT0 to 2 and 0 respectively. As in the previous least squares model, the set of starting values was generated from a truncated multivariate Cauchy( $\boldsymbol{\eta}_1$ , 2), where  $\boldsymbol{\eta}_1$  is a least squares estimate of (12) on

Table 2: Mean, standard deviation, extremes, and quartiles of the objective values for 100 repeated runs of SMC-SA with the reciprocal schedule and CEPSO, on HT1.

Algorithms	Mean	SD	Min	Q1	Q2	Q3	Max
SMC-SA	3.804	0.001	3.803	3.803	3.803	3.804	3.809
CEPSO	4.067	0.606	3.803	3.803	3.804	3.805	5.453

HT1. For the pilot estimate of CEPSO, an unconstrained least squares estimate of (8) on HT1 was used, and was obtained using the Newton-Gauss algorithm starting from  $\boldsymbol{\eta}_1$ . An unconstrained M-estimate can also be used as the pilot estimate, but to obtain this will require a different optimisation method.

Due to the presence of outliers, the estimate obtained from the Newton-Gauss algorithm (the black dotted curve in Figure 2) was a local minimum in the corresponding residual sum of squares function, and thus, when used as the pilot estimate, may lead CEPSO to a local minimum. In fact, 16 out of 100 of the CEPSO runs converged to a local minimum, which is reflected in Table 2 and the apparent departure of the grey curves from the best estimate (black solid line) in the right panel of Figure 2. In contrast, when using SMC-SA, such problems were not apparent with all 100 runs converging to an estimate which appeared to be  $\boldsymbol{\theta}^*$ . Therefore, in such instances, we conclude that SMC-SA is preferable since it does not require a pilot estimate.

## 5. Discussion

We introduce a constrained-augmented SMC-SA algorithm which is capable of optimising with a wide variety of constraints, including those that do

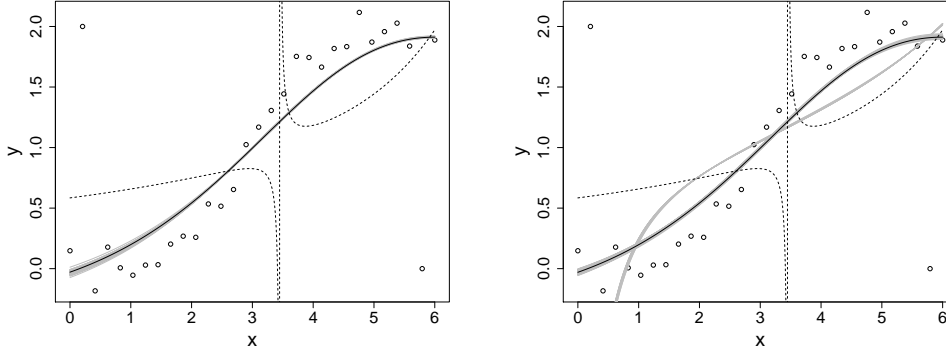


Figure 2: A hundred regression curves (grey) are plotted for SMC-SA and CEPSO. The best estimate obtained from each algorithm is plotted as a black solid curve. The outputs from SMC-SA and CEPSO are shown in left and right panels respectively. The pilot estimate used in this example (black dotted) is problematic as there is a pole between  $x = 3$  and  $x = 4$ .

not have closed-form expressions. The algorithm only requires an indicator function that verifies the feasibility of an estimate to operate, as opposed to CEPSO which requires an additional pilot estimate which may be difficult to obtain.

Our algorithm was built upon the fact that a Boltzmann distribution will converge to a degenerate distribution whose mass is concentrated on the global minimum as the temperature decreases to 0, even when its support is restricted to a subset of a real space. Therefore, we follow the idea of Zhou and Chen (2013) to sample from the sequence of Boltzmann distributions using a SMC sampler.

The running time of our algorithm is mainly concentrated on the rejection sampler that generates proposed states from (6). However, the usage of rejection samplers, which is necessary in our algorithm due to the lack of

assumptions on the nature of the constraints, is notoriously inefficient for truncating high dimensional distributions, particularly when the probability mass of the untruncated (6) is spreading mainly across the infeasible set. For this reason, it is advisable to start the algorithm with a set of feasible starting values to avoid lengthy computation at the first iteration, although our algorithm works with arbitrary starting values in principle. Moreover, when working with a large set of starting values, the computational time can be further improved by parallelising the SA-move, which is executed independently for each  $\gamma_k^j$ .

Although our algorithm is originally intended to solve shape-constrained regression problems, it can be generalised to solve generic constrained optimisation problems. However, one may expect that the reciprocal schedule may be less suitable since the cooling schedule is usually dependent on the problem at hand. In such cases, we advise tweaking the  $\alpha$  in (7) first, before trying an alternative family of cooling schedules when a performance improvement is not immediately attained (Fouskakis and Draper, 2002).

The proposal variance, in particular its decreasing factor, is also crucial to the algorithm convergence. Our motivation of decreasing the variance after each iteration is to maintain a healthy acceptance rate (around 0.2 to 0.5) at the latter stages of the algorithm, when a substantial move from the current states is unlikely to improve the search chain. During that period, the algorithm should focus on refining the current estimates rather than exploring new regions in the parameter space, and a small proposal variance will facilitate this effort. However, the choice of a 3% decrement in our study may be too aggressive in some situations and prevent the algorithm to explore

the parameter space effectively. Hence, the user should adjust the decrement accordingly.

As with all optimisation problems, rescaling of the data is sensible to ensure numerical stability and hence the choice of the scale of our example data, which in turn affects the choice of hyperparameters (i.e. cooling schedule and proposal variance).

## References

Andreani, R., Fukuda, E. H., Silva, P. J. S., 2013. A Gauss–Newton approach for solving constrained optimization problems using differentiable exact penalties. *Journal of Optimization Theory and Applications* 156 (2), 417–449.

URL <http://dx.doi.org/10.1007/s10957-012-0114-6>

Bon, J. J., Murray, K., Turlach, B. A., 2017. Fitting monotone polynomials in mixed effects models. *Statistics and Computing*, 1–20.

Brezger, A., Steiner, W. J., 2008. Monotonic regression based on Bayesian Psplines. *Journal of Business & Economic Statistics* 26 (1), 90–104.

URL <http://dx.doi.org/10.1198/073500107000000223>

Del Moral, P., Doucet, A., Jasra, A., 2006. Sequential Monte Carlo samplers. *Journal of the Royal Statistical Society: Series B (Statistical Methodology)* 68 (3), 411–436.

Elphinstone, C. D., 1983. A target distribution model for nonparametric density estimation. *Communications in Statistics - Theory and Methods*

12 (2), 161–198.

URL <http://dx.doi.org/10.1080/03610928308828450>

Fouskakis, D., Draper, D., 2002. Stochastic optimization: a review. *International Statistical Review* 70 (3), 315–349.

Hastings, W. K., 1970. Monte Carlo sampling methods using Markov chains and their applications. *Biometrika* 57 (1), 97–109.

Hazelton, M. L., Turlach, B. A., 2011. Semiparametric regression with shape-constrained penalized splines. *Computational Statistics & Data Analysis* 55 (10), 2871–2879.

Huber, P. J., 1981. *Robust Statistics*. John Wiley & Sons, Inc., New York.

Kelly, C., Rice, J., 1990. Monotone smoothing with application to dose-response curves and the assessment of synergism. *Biometrics* 46 (4), 1071–1085.

URL <http://www.jstor.org/stable/2532449>

Kirkpatrick, S., Gelatt, Jr., C. D., Vecchi, M. P., 1983. Optimization by simulated annealing. *Science* 220 (4598), 671–680.

URL <http://dx.doi.org/10.1126/science.220.4598.671>

Leitenstorfer, F., Tutz, G., 2007. Generalized monotonic regression based on B-splines with an application to air pollution data. *Biostatistics* 8 (3), 654–673.

URL <http://dx.doi.org/10.1093/biostatistics/kxl036>

- Locatelli, M., 2000. Simulated annealing algorithms for continuous global optimization: convergence conditions. *Journal of Optimization Theory and applications* 104 (1), 121–133.
- Locatelli, M., 2002. Simulated annealing algorithms for continuous global optimization. In: *Handbook of global optimization*. Springer, pp. 179–229.
- Manderson, A. A., Cripps, E., Murray, K., Turlach, B. A., 2017. Monotone polynomials using BUGS and Stan. *Australian & New Zealand Journal of Statistics* 59 (4), 353–370.
- Marsh, H., 1980. Age determination of the dugong (*Dugong dugon* (Muller)) in northern Australia and its biological implications. Zoology Department, James Cook University of North Queensland.
- Matzkin, R. L., 1991. Semiparametric estimation of monotone and concave utility functions for polychotomous choice models. *Econometrica* 59 (5), 1315–1327.  
URL <http://www.jstor.org/stable/2938369>
- Metropolis, N., Rosenbluth, A. W., Rosenbluth, M. N., Teller, A. H., Teller, E., 1953. Equation of state calculations by fast computing machines. *The Journal of Chemical Physics* 21 (6), 1087–1092.
- Meyer, M. C., 2012. Constrained penalized splines. *Canadian Journal of Statistics* 40 (1), 190–206.  
URL <http://dx.doi.org/10.1002/cjs.10137>
- Meyer, M. C., Hackstadt, A. J., Hoeting, J. A., 2011. Bayesian estimation

- and inference for generalised partial linear models using shape-restricted splines. *Journal of Nonparametric Statistics* 23 (4), 867–884.
- Murray, K., Müller, S., Turlach, B. A., 2013. Revisiting fitting monotone polynomials to data. *Computational Statistics* 28 (5), 1989–2005.  
URL <http://dx.doi.org/10.1007/s00180-012-0390-5>
- Murray, K., Müller, S., Turlach, B. A., 2016. Fast and flexible methods for monotone polynomial fitting. *Journal of Statistical Computation and Simulation* 86 (15), 2946–2966.  
URL <http://dx.doi.org/10.1080/00949655.2016.1139582>
- Newman, D. J., 03 1964. Rational approximation to  $|x|$ . *The Michigan Mathematical Journal* 11 (1), 11–14.  
URL <http://dx.doi.org/10.1307/mmj/1028999029>
- Nocedal, J., Wright, S. J., 2006. *Numerical Optimization*, 2nd Edition. Springer Series in Operations Research and Financial Engineering. Springer, New York.
- Nourani, Y., Andresen, B., 1998. A comparison of simulated annealing cooling strategies. *Journal of Physics A: Mathematical and General* 31 (41), 8373.  
URL <http://stacks.iop.org/0305-4470/31/i=41/a=011>
- Piegorsch, W. W., Bailer, A. J., 2005. *Nonlinear Regression*. John Wiley & Sons, Ltd, Ch. 2, pp. 83–87.  
URL <http://dx.doi.org/10.1002/0470012234.ch2>

- Pyra, N., Wood, S. N., May 2015. Shape constrained additive models. *Statistics and Computing* 25 (3), 543–559.  
URL <https://doi.org/10.1007/s11222-013-9448-7>
- R Core Team, 2018. R: A Language and Environment for Statistical Computing. R Foundation for Statistical Computing, Vienna, Austria.  
URL <https://www.R-project.org/>
- Ralston, A., Rabinowitz, P., 1978. A first course in numerical analysis, 2nd Edition. McGraw-Hill Book Co., New York-Auckland-Bogotá, international Series in Pure and Applied Mathematics.
- Ramsay, J. O., 1998. Estimating smooth monotone functions. *Journal of the Royal Statistical Society: Series B (Statistical Methodology)* 60 (2), 365–375.  
URL <http://dx.doi.org/10.1111/1467-9868.00130>
- Reddi, S. J., Hefny, A., Downey, C., Dubey, A., Sra, S., 2015. Large-scale randomized-coordinate descent methods with non-separable linear constraints. In: *Proceedings of the Thirty-First Conference on Uncertainty in Artificial Intelligence. UAI'15*. AUAI Press, Arlington, Virginia, United States, pp. 762–771.  
URL <http://dl.acm.org/citation.cfm?id=3020847.3020926>
- Romeijn, H. E., Smith, R. L., Sep 1994. Simulated annealing for constrained global optimization. *Journal of Global Optimization* 5 (2), 101–126.  
URL <https://doi.org/10.1007/BF01100688>

Thornley, J. H. M., 1999. Modelling stem height and diameter growth in plants. *Annals of Botany* 84 (2), 195.

URL <http://dx.doi.org/10.1006/anbo.1999.0908>

Wolters, M. A., 2012. A particle swarm algorithm with broad applicability in shape-constrained estimation. *Computational Statistics & Data Analysis* 56 (10), 2965–2975.

Zhou, E., Chen, X., 2013. Sequential Monte Carlo simulated annealing. *Journal of Global Optimization* 55 (1), 101–124.

URL <http://dx.doi.org/10.1007/s10898-011-9838-3>